

LETTER • OPEN ACCESS

Reassessing hourly precipitation–temperature scaling: the diurnal cycle in a warming China

To cite this article: Miao Lei et al 2025 Environ. Res. Lett. 20 024006

View the article online for updates and enhancements.

You may also like

- A framework for modeling carbon loss from rivers following terrestrial enhanced weathering
- Shuang Zhang, Christopher T Reinhard, Shaoda Liu et al.
- <u>Direct and semi-direct aerosol effects on the scaling of extreme sub-daily precipitation over East China</u>
 Shuping Li, Tao Su, Ruolan Xiang et al.
- Beneficial role of diurnal smoothing for grid integration of wind power
 Anasuya Gangopadhyay, Ashwin K Seshadri and Ralf Toumi



ENVIRONMENTAL RESEARCH

LETTERS



OPEN ACCESS

RECEIVED

23 September 2024

REVISED 12 December 2024

ACCEPTED FOR PUBLICATION

30 December 2024

10 January 2025

Original content from this work may be used under the terms of the Creative Commons Attribution 4.0 licence.

Any further distribution of this work must maintain attribution to the author(s) and the title of the work, journal citation and DOI.



LETTER

Reassessing hourly precipitation-temperature scaling: the diurnal cycle in a warming China

Miao Lei, Shanshan Wang b, Jianping Huang, Zhiyang Wang and Xiaoping Li

Key Laboratory for Semi-Arid Climate Change of the Ministry of Education, College of Atmospheric Sciences, Lanzhou University, Lanzhou, People's Republic of China

Author to whom any correspondence should be addressed.

E-mail: wangss@lzu.edu.cn

Keywords: Clausius-Clapeyron (CC) relationship, Diurnal variations, Interannual variation, Hourly precipitation Supplementary material for this article is available online

Abstract

Hourly extreme precipitation is expected to intensify with global warming following a Clausius—Clapeyron (CC) relationship. While extensive research has investigated the relationship between hourly precipitation and temperature, inconsistencies in this relationship across the diurnal cycle affect all-hours scaling. This study uses hourly gauge observations and reanalysis data from mainland China to analyze the scaling and explore its diurnal cycle for the first time. Our results reveal that 88.7% of the stations exhibit super-CC scaling, which is significantly underestimated by reanalysis data. Notably, the scaling shows a pronounced diurnal cycle and exceeds all-hour scaling, indicating that the mix of precipitation from different hours ultimately affects the overall scaling results. Over a 39 year period, changes in extreme precipitation intensity were closely aligned with dew-point temperatures throughout the diurnal cycle in inland regions. The above results provide a valuable insight into the shift of extreme precipitation to morning/night in some regions under climate change.

1. Introduction

With global warming, extreme precipitation intensity (EPI) is projected to increase significantly in the future (Craig 2010, Lehmann et al 2015, Chen et al 2021). This trend largely follows a Clausius-Clapeyron (CC) relationship, which posits that the moisture-holding capacity of the atmosphere increases by approximately 7% for every degree of warming when relative humidity (RH) remains relatively constant. This increase, in turn, supports heavier precipitation intensity. Correspondingly, extreme precipitation is expected to respond to warming at a rate of 7%/K, due to EPI mainly determined by the precipitable water in the atmosphere. This enhanced extreme precipitation has the potential to trigger floods, debris flows and urban waterlogging, thereby threatening socio-economic infrastructures and causing loss of life (Vogel et al 2019, Liu et al 2021). Moreover, given the relatively greater confidence in predicting future temperatures than in forecasting extreme precipitation (Johnson and Sharma

2009, Tian et al 2017), many studies have attempted to estimate how extreme precipitation has responded to temperature in the past, often referred as to 'scaling', and use this relationship to provide insights into future changes in extreme precipitation (Lenderink and Attema 2015, Wang et al 2018). Therefore, it is critical to understand how changes in extreme precipitation respond to increasing temperature to mitigate future climate risks.

Previous studies have found significant variability in how extreme precipitation scales with temperature, ranging from negative CC to super CC scaling based on gauge observations and reanalysis, particularly in warm climatic regions where negative scaling is commonly reported (Utsumi et al 2011). These deviations can be attributed to multiple factors, including precipitation type (Berg et al 2013), large-scale circulations (Blenkinsop et al 2015), the duration of precipitation events (Hatsuzuka et al 2021), seasonal temperature variations (Berg et al 2009) and aerosol indirect effects (Da Silva et al 2020). Additionally, the accuracy of precipitation data, the methodology used to

estimate scaling (Boessenkool et al 2017, Ali et al 2022) and the choice of temperature variable (Bui et al 2019) are crucial considerations. Other important factors include the source (Ali et al 2022, Moustakis et al 2020) and temporal scale of precipitation data (Xiao et al 2016, Wang et al 2018). Reanalysis data sets such as ERA5 and MERRA2 are the the most commonly used, alongside gauge observations, helping to extend scaling research over regions with sparse gauge data by providing broader coverage for extreme precipitation scaling studies (Sun et al 2018). However, existing research indicates that the scaling estimates derived from these two reanalysis datasets are lower than those obtained at station level in places such as the USA and Japan (Moustakis et al 2020, Ali et al 2021). Despite this, a comprehensive evaluation of reanalysis data against observations in China remains lacking.

In terms of temporal scale, previous studies have indicated that while daily precipitation increases with temperature in accordance with CC scaling (Roca 2019), sub-daily extreme precipitation in certain regions often increases at a rate exceeding 7%/K, known as super-CC scaling (Lenderink and Van Meijgaard 2008, Wang et al 2018). Additionally, in Eastern China, daily precipitation has been shown to exhibit negative scaling with daily mean temperature, contrasting with the positive scaling observed for hourly data (Xiao et al 2016). This discrepancy may be attributed to sub-daily extreme precipitation mainly resulting from convective rainfall occurring in the afternoon, while daily extreme precipitation often involves long-duration events in the early morning at low temperatures. Although many studies mentioned above have investigated the relationship of hourly precipitation scaling to temperature, the diurnal cycle of scaling has received limited attention (Meredith et al 2019, 2021). This aspect could significantly influence the overall scaling and alter diurnal patterns of extreme precipitation in the future, thereby providing better scientific support for decision-makers in extreme precipitation prevention.

To address the identified knowledge gaps, this study aims to answer the following questions: (1) can reanalysis data accurately reproduce the scaling behavior observed in mainland China? (2) What are the characteristics of the diurnal cycle of this scaling in mainland China? We utilize hourly precipitation and dew point temperature (DPT) data from ground-based stations and reanalysis sources to clarify the scaling behavior across mainland China. This study will be the first to examine the diurnal cycle of scaling from an observational perspective and will determine how long-term variations in extreme precipitation correspond to long-term shifts in DPT throughout the diurnal cycle.

2. Datasets and methodology

2.1. Ground-based hourly precipitation data

In this study, we used 1980–2018 hourly precipitation data from May to September (warm season) in mainland China obtained from the China Meteorological Administration. To ensure a sufficient amount of data, only stations with at least 12 years of observation records and an annual missing rate of less than 10% were retained for the analysis. Due to the limited sensitivity of the surface observation instruments, the minimum observed value of surface precipitation is recorded as 0.1 mm h^{-1} (Oin et al 2021, Lei et al 2022). High-precision and quality-controlled precipitation data can reduce the uncertainty of scaling (Ali et al 2022). Considering water vapor limitations at higher temperatures can lead to negative scaling outcomes, especially in warmer regions (Berg et al 2009, Barbero et al 2018). Compared to surface temperature, DPT has been used as a better scaling variable, as it directly measures atmospheric absolute humidity (Wasko et al 2018). Before automatic meteorological observations were established, hourly precipitation data were transformed from a self-recorded precipitation paper, with DPT observed only four times a day at 02:00, 08:00, 14:00 and 20:00 Beijing time (BJT). We used the nearest DPT before the precipitation hour to match precipitation temperature pairs, due to temperature anomalies being lower after precipitation events had occurred (Visser et al 2020). If there was another precipitation event between the initial precipitation and the nearest DPT (with an event separation time of 1 h), that precipitation was excluded from the matching process for precipitation-temperature pairs. We also used daily DPT as a scaling variable for comparison with DPT measured at 6 h intervals. Daily DPT was calculated from daily temperature (T) and RH as follows (Guo et al 2020):

$$DPT = RH(A + B \times T) + C \times T - 19.2 \tag{1}$$

where A = 0.198, B = 0.0017 and C = 0.84.

2.2. Reanalysis datasets

In this work, we applied two sets of advanced reanalysis products: ERA5 and MERRA2 (Gelaro *et al* 2017, Hersbach *et al* 2018). ERA5 and MERRA2 provide long-term global hourly meteorological data that complement many regions lacking observational data. We used hourly precipitation and DPT data from ERA5 and MERRA2 for the period 1980–2018 to evaluate whether reanalysis data can reproduce the scaling behavior observed in mainland China. Reanalysis data were interpolated to the station via the inverse distance weighting method (Li and Heap 2008). We ignored light precipitation <0.1 mm h⁻¹

in the reanalysis data in order to be consistent with observations. It is worth noting that although hourly DPT data were available from the reanalysis data, precipitation—DPT pairs were constructed using methods consistent with those applied to the observations (hourly precipitation matching only DPT at 2:00, 8:00, 14:00 and 20:00 BJT).

2.3. Methods

The binning method was used to estimate 'binning scaling' (Lenderink and Van Meijgaard 2008, Zhang et al 2017). Since equal-size temperature bins may cause empty or an insufficient number of data bins, influencing the relationship between precipitation and temperature (Herath and Sarukkalige 2018), the DPT–precipitation pairs were first distributed into 12 bins of equal-sample size from low to high DPT. The first and last bins were excluded to remove abnormal DPT caused by specific atmospheric circulation (Ali et al 2021, Hosseini-Moghari and Tang 2022). The mean DPT and the 99th quantile of precipitation (P_{99}) for wet hours ($P \ge 0.1 \text{ mm h}^{-1}$) in each bin were calculated, and the line regression was fitted using equation (2):

$$ln(P_{99}) = \alpha(\overline{DPT}) + \beta.$$
(2)

 α and β were regression coefficients determined by line regression. The scaling $\frac{\partial P_{99}}{\partial \overline{\rm DPT}}$ was calculated as follows:

$$\frac{\partial P_{99}}{\partial \overline{\text{DPT}}} = 100\% \times (e^{\alpha} - 1) \tag{3}$$

where $\overline{\mathrm{DPT}}$ is mean DPT in each bin.

The regional scaling results were calculated by pooling data from all stations. To further explore the diurnal variation in scaling, we applied the same methodology to calculate the scaling for four time periods, each containing 3 h of precipitation data. This approach allowed us to examine the diurnal cycle of scaling throughout the day.

3. Results and discussion

Initially, we estimated the scaling of hourly extreme precipitation paired with DPT using observations, as well as the ERA5 and MERRA2 datasets for mainland China. A total of 98.33% of stations showed positive scaling based on observations, while the remaining stations with negative scaling were mainly concentrated in northwest China (NWC) and southern China (see figure 1(a)). In terms of scaling magnitude, 48.16% and 40.61% of the stations exhibited scaling greater than 2CC (14%/K) and 1CC (7%/K), respectively. When daily mean DPT was used as the variable for studying scaling (figure S1), the spatial distribution was similar to that observed using surface temperature in previous reports (Xiao *et al* 2016). The

number of stations with negative scaling using 6 h DPT deceased from 2.63% to 1.67% of all stations, and the percentage of stations where scaling exceeded 14%/K increased by 6.7% compared to those using the daily mean DPT. This is because using daily mean DPT can be affected by temperature anomalies following precipitation events, causing an underestimation of scaling in mainland China. The surrounding distribution of ocean and land, along with variations in latitude across different regions, is a major factor contributing to regional scaling differences. In central and eastern China, stations showed super-CC scaling, which may be related to the enhancement of convective activity through latent heat release (Lenderink and Van Meijgaard 2008) or changes in precipitation type (Berg et al 2013). Notably, stations in the NWC and Qinghai-Tibet Plateau (TP) regions, which have received less attention in previous studies, mainly display negative and sub-CC scaling. This implies that extreme precipitation in arid and semi-arid regions is less sensitive to DPT. This finding aligns with the results observed in the Mediterranean's arid and semiarid regions (Pumo and Noto 2021), likely due to moisture availability limitations in the arid region. In particular, the low afternoon RH further restricts the scaling relationship, highlighting the importance of considering the diurnal cycle in scaling research.

Reanalysis data significantly underestimate the scaling of extreme precipitation in mainland China, with 10.9% and 17.6% of stations showing negative scaling mainly located in the tropical and subtropical regions of southern China according to both ERA5 (figure 1(b)) and MERRA2 (figure 1(c)), respectively. Additionally, over two-thirds of the stations exhibit sub-CC scaling, with the remaining stations displaying super-CC scaling. A similar spatial pattern is also observed for the more extreme percentile (99.9th) (figure S2). In particular, ERA5 underestimates the average scaling of 9.4%/K observed in actual measurements, especially for stations in southern China where high DPT conditions lead to a negative scaling, which is completely inconsistent with observations. The high temperatures in the reanalysis data can increase the saturation deficit, which slows down the cumulus updraft condensation and ultimately leads to negative scaling (Sun and Wang 2022). The scaling derived from MERRA2 is even lower than that from ERA5. However, on Hainan Island, stations measured with MERRA2 exhibit super-CC scaling, whereas ERA5 and observations occasionally show negative or sub-cc scaling. When examining the scaling behavior on Hainan Island across the three datasets (see figure S3), discrepancies become apparent. Although some stations show negative scaling based on observations, regional averaging reveals a scaling rate close to the CC rate. MERRA2 gives a scaling near 2CC but seriously underestimates the precipitation intensity. ERA5 captures a relatively strong intensity but

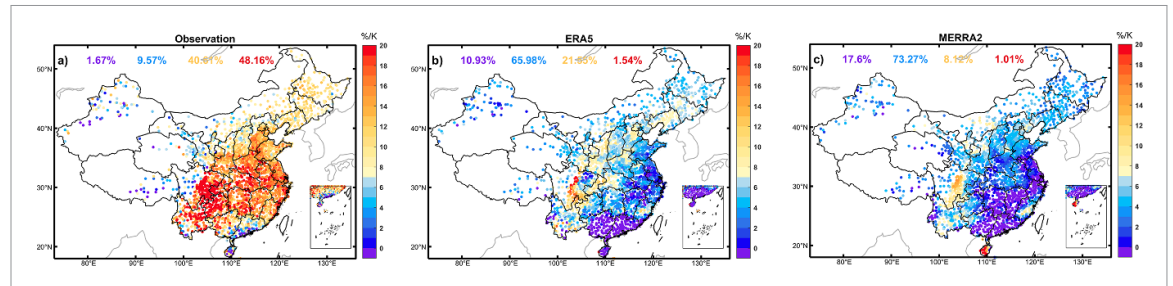


Figure 1. Distribution of the scaling of the 99th percentile, using estimates derived from hourly precipitation data and 6-hourly dew point temperature (DPT) from observations (a), ERA5 (b) and MERRA2 (c). The numbers at the top of the panels represent the proportion of stations within each interval (purple numbers represent the proportion of sites with negative scaling, blue represents scaling between 0 and 1CC, orange represents scaling between 1CC and 2CC, and red represents more than 2CC).

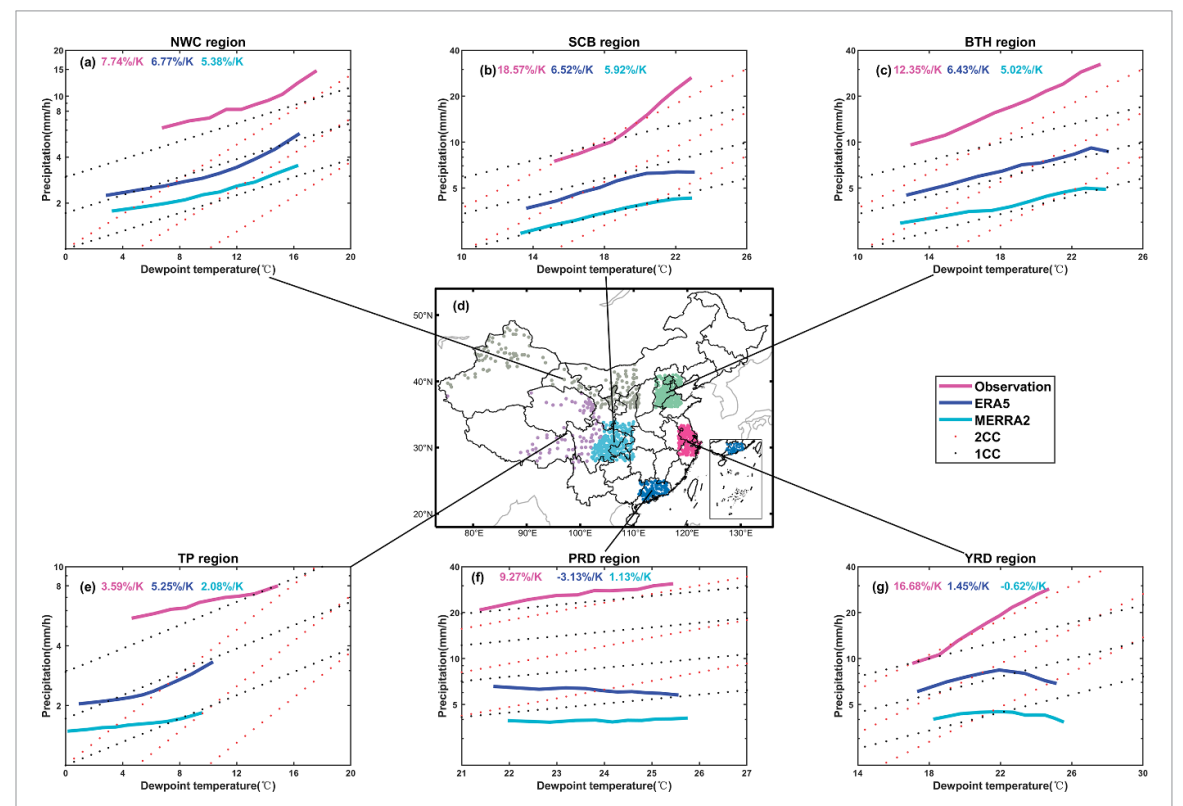


Figure 2. (a)–(c), (e)–(g) The relationships between the 99th percentile and the DPT of six regions from observations (magenta), ERA5 (indigo blue) and MERRA2 (pale blue). The numbers in the upper-right corner of each panel represent the scaling rate for that region. The dashed lines represent a 2CC (red) and CC (grey) increase. In panel (d), different colors are used to represent the six regions.

shows a consistent decrease, with a scaling -4.2%/K. The main reason for the discrepancies between the reanalysis data and observations lies in the reanalysis data's inadequate modeling of extreme precipitation, especially significant underestimation of convective precipitation intensity (Aleshina *et al* 2021), rather than temperature (Ali *et al* 2021). Reanalysis data severely underestimate the scaling of hourly precipitation in China, with over half of stations showing sub-CC scaling, compared to approximately 90% stations demonstrating super-CC scaling from observations. This stark contrast suggests that the observed data capture a more pronounced response of short-term extreme precipitation to changes in DPT during the warm season. This pattern may not be accurately

reflected in the reanalysis data but could be more precise during the winter (Aleshina *et al* 2021).

The scaling relationship between precipitation extremes and DPT exhibits significant geographic variation across China (figure 1), as highlighted by Guo *et al* (2020). To examine this scaling behavior in different regions, six typical regions were selected for analysis, as shown in figure 2(d): the Sichuan Basin (SCB), Beijing–Tianjin–Hebei (BTH), the Yangtze River Delta (YRD), the Pearl River Delta (PRD), the TP and NWC. We first constructed temperature–precipitation curves to visualize the scaling relationship across for the full DPT range of these six regions. Observational data revealed a positive scaling in all regions without any 'hook' structure, with the highest

extreme precipitation coinciding with the highest DPT. In the NWC region (figure 2(a)), precipitation intensity increases monotonically with DPT, showing nearly a 7%/K scaling rate. However, the curves from ERA5 and MERRA2 were biased toward cooler temperatures and consistently underestimated the precipitation intensity across all temperature ranges in the NWC region. Observational scaling in the SCB exceeds 14%/K (figure 2(b)), with near-CC scaling under a DPT of 20 °C and over 2CC scaling above 20 °C. In contrast, the reanalysis data here show near-CC scaling but exhibited a 'hook' structure at high DPT levels. For the BTH region, the observational data exhibited super-CC, whereas the reanalysis data showed flat and hook structures with underestimation above 22 °C (figure 2(c)). In the TP region, although sub-CC scaling was observed (figure 2(e)), EPI nonetheless rose with temperature. Reanalysis data underestimated DPT during precipitation by about 5 °C compared to the observed values, yet still reflected sub-CC scaling consistent with observations. In the PRD region, where a 'hook' structure in precipitation-temperature relationships was previously documented by Sun et al (2015), we found that using DPT before precipitation as temperature variable eliminated this 'hook' structure in the regional scaling curve (figure 2(f)). Additionally, pooling data from stations with partial positive scaling tended to mask the regional negative scaling observed at some stations, similar to the pattern in the NWC region. The YRD region showed a clear divergence between observations and reanalysis (figure 2(g)): observed data increased monotonically, following a 2CC rate across all temperatures, whereas reanalysis data exhibited a pronounced 'hook' structure at a peak point temperature of 22 °C. Notably, MERRA2 and ERA5 noticeably underestimated EPI across all regions and temperature ranges, especially at high DPT levels. Combining these findings, it becomes evident that in reanalysis data across regions, extreme precipitation increases with DPT at low DPT ranges (<22 °C), but decreases or levels off at high DPT ranges (>22 °C). This explains why some stations in southern China with high DPT show negative scaling in ERA5 and MERRA2, highlighting that reanalysis data for China's warm season fail to reflect the results from observations accurately. Similar findings have been observed for the 99.9th percentile (figure

The results presented above were derived from pooling all precipitation–DPT paired data across all hours, without considering the diurnal cycle. However, it is important to recognize that extreme precipitation exhibits diurnal variation (figure S5). Most regions, such as NWC, BTH, YRD and PRD, show an afternoon peak in observations, while the SCB was characterized by nocturnal rainfall with higher extreme precipitation intensities at night. The

peak value occurs in the early morning in most regions based on reanalysis data, which is inconsistent with observations. Precipitation at low DPT levels usually occurs in the early morning, contributing significantly to the low-temperature portion of the precipitation-temperature curve. In contrast, afternoon precipitation, associated with higher temperatures, constructs the high-temperature portion of the curve. To address confounding effects, we calculated scaling based on observation for four time periods, 2:00-5:00, 8:00-11:00, 14:00-17:00 and 20:00-23:00 after DPT observations (figure 3). The results for the reanalysis data are presented in figure S6. Due to the poor performance of all-hours scaling and the extreme precipitation diurnal cycle pattern, we mainly focus on observational perspectives for further analysis. This helps illuminate the sensitivity of extreme precipitation to DPT at the diurnal cycle scale. Our analysis revealed significant diurnal variations, indicating that the mix of precipitation from different hours ultimately affects the overall scaling.

In both the NWC (figure 3(a)) and BTH (figure 3(c)) regions, we observed higher scaling at 2:00–5:00 and 8:00–11:00, and lower scaling at 14:00– 17:00 and 20:00-23:00. This pattern suggests that extreme precipitation occurring at night and in the morning is more sensitive to changes in DPT compared to those occurring in the afternoon and evening. This may be because air tends to be much closer to saturation during these times of the day, leading to lower dewpoint depression. Under certain meteorological conditions, cooling the air to saturation can suffice to trigger convection, thereby supporting super-CC scaling, as highlighted by Siswanto et al (2022). The diurnal cycle of extreme precipitation in these two regions exhibited a bimodal structure, with a main peak occurring in the afternoon and a secondary peak in the early morning (figure S5). Our findings suggest that the sub-peak in the early morning may strengthen and reduce the difference from the main peak in the afternoon under climate change. This further supports the idea that future extreme precipitation may shift from afternoon to night and morning, as suggested by the convection-permitting model (Meredith et al 2019). In the SCB region, the diurnal variation region was less pronounced, with peak scaling at 2:00-5:00 (figure 3(b)). However, the more extreme percentile (99.9th) also shows a similar pattern (figure S7(b)), consistent with the NWC and BTH regions. In contrast, the YRD region exhibited an opposing pattern from the NWC and BTH regions (figure 3(f)), with scaling proximity 20%/K at 14:00– 17:00, but dropping below at other time periods. The extreme precipitation diurnal cycle in the YRD region showed a single-peak structure occurring in the afternoon (figure S3). This suggests that the main peak may strengthen and significantly influence the diurnal cycle of extreme precipitation under a warmer

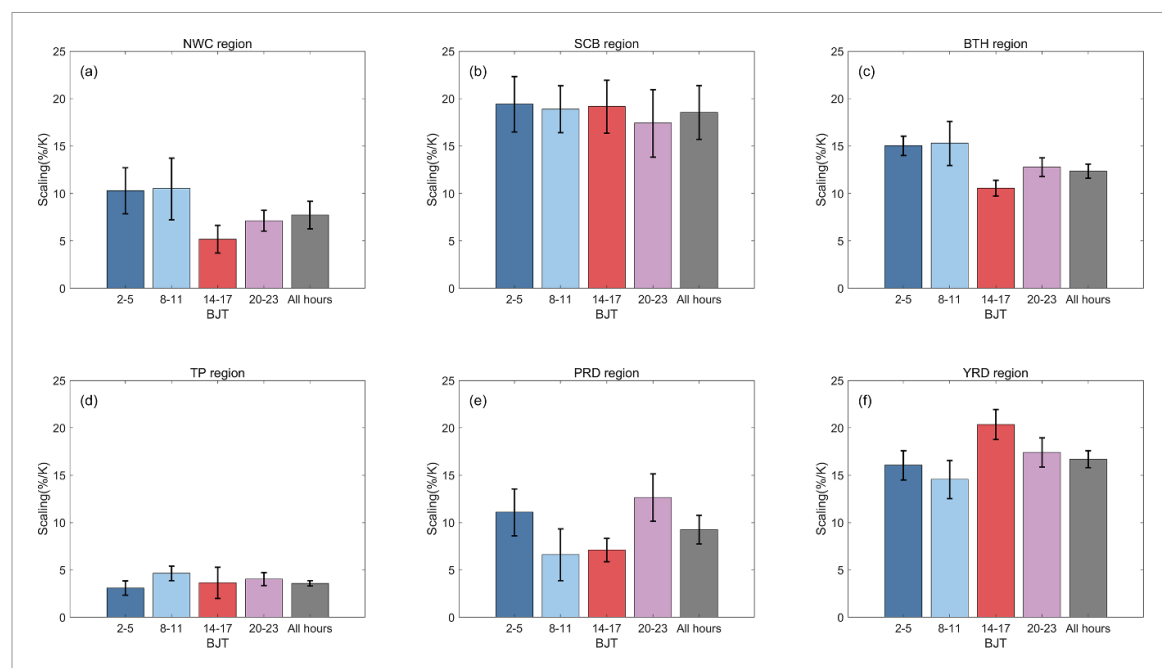


Figure 3. The scaling of the 99th percentile of BJT 2:00–5:00, 8:00–11:00, 14:00–17:00 and 20:00–23:00 and all-hours scaling for the NWC (a), SCB (b), BTH (c), TP (d), PRD (e) and YRD (f) regions. The plot of each bar represents the 95% confidence interval of the scaling rate.

climate. Meanwhile, the TP region consistently displayed sub-CC scaling across all hours (figure 3(d)), indicating a weak response of extreme precipitation to temperature increase in this region. Although the all-hours scaling in the PRD region was comparable to that in the NWC region, the diurnal cycle showed a distinct pattern, peaking at exceed 11%/K at 2:00– 5:00 and 20:00-23:00. This suggests an enhancement of extreme precipitation during the night in the PRD area. Peak precipitation in this region occurs during the afternoon, indicating that significant diurnal variability may diminish in the future. These results imply that the response of extreme precipitation to DPT exhibits significant diurnal cycles, the scaling of special time periods may exceed the all-hours scaling, supporting that the diurnal precipitation pattern may alter under climate change effects. The results from ERA5 and MERRA-2 exhibited similar scaling as the all-hours results in most regions, except for the PRD region (figure S6), the reanalysis data ineffectively reproduce the diurnal cycle pattern in observations. Furthermore, as the diurnal temperature range exhibits obvious temporal and spatial variations (Wang et al 2024), using temperature with a diurnal cycle instead of daily mean temperature as predictive factors may more accurately represent the atmospheric water vapor conditions related to precipitation in the future.

For each region, the logarithm of the 99th percentile hourly precipitation intensity for four time periods was plotted against DPT based on observations, as shown in figure 4. The NWC region exhibits higher scaling at 2:00-5:00 and 8:00-11:00, primarily because the curves at these times show low EPI at a low DPT range, while all curves converge to similar EPI values at higher DPT ranges. Similarly, the BTH region exhibits results comparable to those of the NWC region, with the curves at 2:00-5:00 and 8:00–11:00 following the 2CC rate across all temperature ranges. In contrast, the curves at 14:00-17:00 and 20:00-23:00 adhere to the 2CC rate at low temperatures but diverge from it above 18 °C. In the SCB region, the nighttime precipitation intensity is higher than at other hours across almost all temperature ranges, deriving the highest scaling at night. In the TP region, sub-CC scaling is observed for all time periods, but exhibits near CC scaling for the 99.9th percentile extreme precipitation (figure S8(d)). The highest extreme precipitation occurs at 20:00-23:00 across all temperature ranges. This aligns closely with the local precipitation diurnal cycle (Wu et al 2018). The extreme precipitation in the TP region responds weakly to temperature, potentially due to its complex topography (Guo et al 2014). The curve in the PRD region oscillates above 23 °C while maintaining an upward trend, with DPT intervals significantly smaller than in other region—often less than 0.5 °C above 23 °C—resulting in unstable oscillations in the curve; the curve shows super-CC scaling at nighttime but closely aligns with the CC rate during daytime. The YRD region reaches approximately 15%/K scaling at 2:00-5:00 and 8:00-11:00, escalating to around 20%/K at 14:00–17:00 (figure 4(f)); all curves exhibit a monotonic increase in EPI with DPT, exceeding the

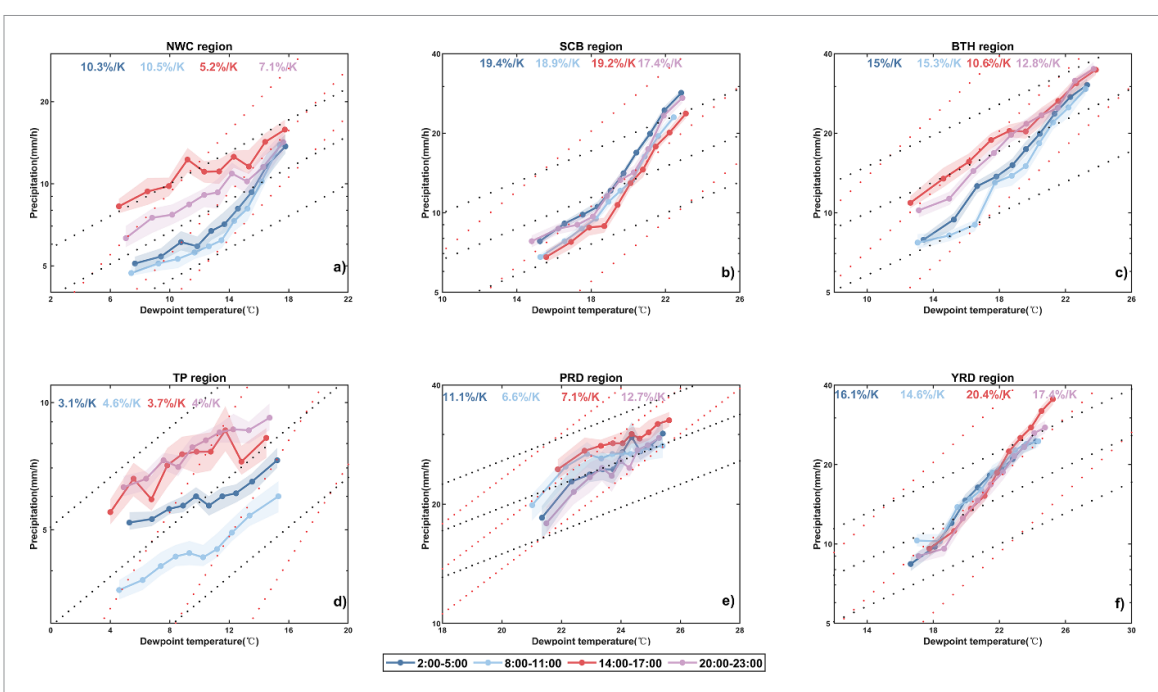


Figure 4. Dependencies of 99th percentiles of extreme precipitation intensity on dew point temperature for four time periods in six regions. The shading indicates 95% confidence intervals for 1000 bootstrap resampling, the dashed lines represent 2CC (red) and CC (grey) increases.

2CC rate across all temperature ranges. The curves from different time periods exhibited a clear precipitation inconsistent response to DPT, indicating that mixing precipitation from different time periods has a great impact on calculate all-hours bin scaling. The 99.9th percentile results display similar discrepancies across time periods, but with a wider confidence interval (figure S8).

To assess whether the variations in extreme precipitation correspond to the variations in DPT across the diurnal cycle scale, we selected data from stations with 39 years of continuous observations and examined the correlation coefficient (*R*) between the annual hourly EPI (99th percentile) for each time period and the annual mean DPT at corresponding hour variations after de-trending across six regions (figure 5). R values were generally high in the four inland regions, indicating that EPI positively covaries with DPT variation across the diurnal cycle. However, low R values were observed in the PRD and YRD regions. In the NWC region, correlations ranging from 0.41 to 0.52 were found across all time periods, with a P-value < 0.05 (figure 5(a)), indicating that more extreme precipitation is often accompanied by higher DPT from inter-annual variation. This highlights the importance of DPT as a predictor of EPI in arid and semi-arid regions. The SCB region showed R values from 0.33 to 0.46 (P-value <0.05) demonstrating a significant correlation between EPI and DPT variations across the diurnal cycle. In the BTH region, the correlation coefficients for four time periods in the BTH region were 0.28, 0.31, 0.37 and 0.24, respectively; these values still exhibit relatively high

significance with a P-value <0.1, except for 20:00-23:00. The TP region also showed fairly high R values with a P-value <0.1, except at 8:00–11:00, where the weaker correlation may stem from limited stations with 39 years of continuous observations and a low frequency of precipitation, resulting in insufficient precipitation data for a robust correlation. Inland regions showed significant correlations between EPI and DPT annual variability, suggesting that interannual variations in extreme precipitation can be better explained by changes in DPT, even on a diurnal scale. In contrast, coastal regions such as the PRD and YRD regions show relatively low R values. Previous studies also noted a lack of obvious correspondence between EPI and DPT in southern China (Guo et al 2020). The changes in hourly extreme precipitation could be related to other reasons, such as urbanization (Yan et al 2024) or shifts in large-scale circulation (Ning et al 2017). Nonetheless, correlations between EPI and DPT at the diurnal scale showed a P-value <0.1 at 14:00–17:00 in the YRD region, suggesting that the PRD region exhibits a reasonable correspondence at a specific time period when considering the diurnal cycle. Reanalysis data also reveal a significant correlation in inland regions, while coastal regions exhibit lower R values, MERRA-2 exhibited higher correlation value than ERA5 in inland region (figure S9).

Our results suggest that the inter-annual variations in hourly extreme precipitation are closely associated with DPT changes on a diurnal scale in some regions. This finding further implies that the diurnal cycle of the scaling relationship can provide

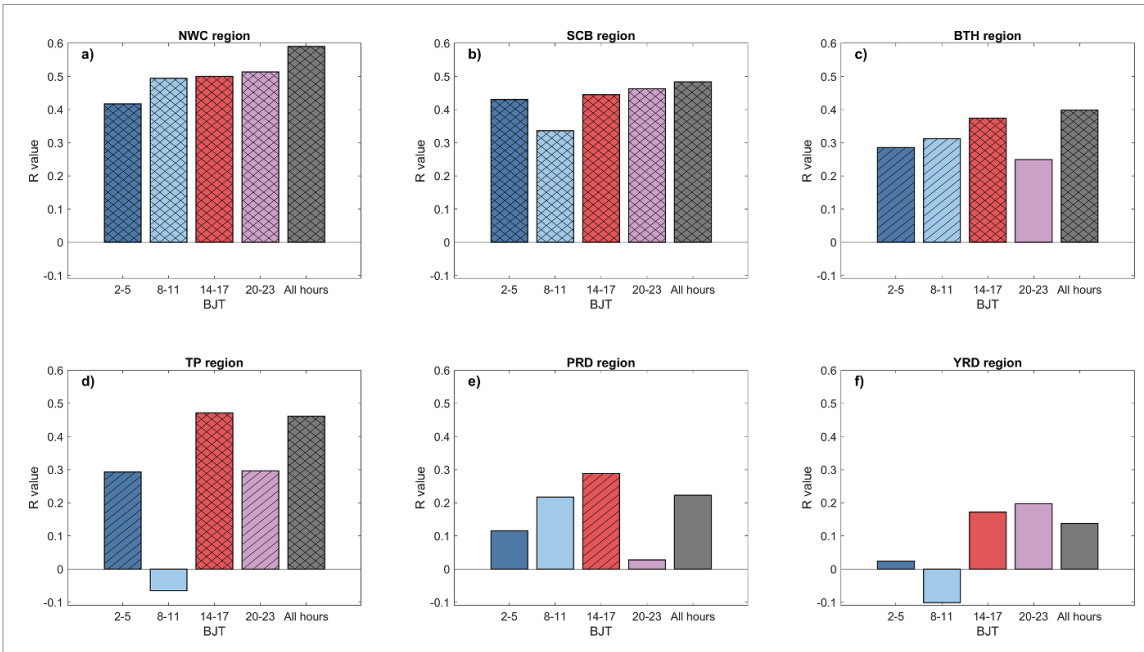


Figure 5. The correlation coefficient between EPI (99th) and annual mean DPT at corresponding hours during 1980–2018 in China for four time periods across six regions. The bar covered by double diagonal lines represents a P-value <0.05, while the bar covered by single diagonal line represents a P-value <0.1.

alternate evidence for future changes in the extreme precipitation diurnal cycle, especially since current region and global climate models struggle to simulate sub-daily extreme precipitation mainly caused by convective active (Hanel and Buishand 2010, Sun *et al* 2020). This limitation is also a key reason for the poor performance of reanalysis data.

4. Conclusions

In this study, we utilized hourly precipitation and DPT data from in situ gauge observations, as well as ERA5 and MERRA2 datasets, during the warm season across mainland China to derive the bin scaling relationship and, for the first time, explore the diurnal cycle of scaling from observations, which has received limited attention in previous studies. This focus is critically important because the mixing of extreme precipitation from different hours affects all-hours scaling and provides alternative evidence for future changes in the diurnal cycle of extreme precipitation. Our observations indicate that 88.7% of stations exhibit super-CC scaling with notable regional differences, influenced by a complex interplay of factors that merit further detailed investigation in our next work. Additionally, the EPI increases monotonically with DPT and no 'hook' structure is observed in the regional scaling curve. However, ERA5 and MERRA2 predominantly show stations with sub-CC scaling, and exhibited a 'hook' structure at DPT about 22 °C in regional scaling curve, suggesting that reanalysis

datasets underestimate changes in hourly extreme precipitation in response to DPT.

By investigating the diurnal cycle from observations, we reveal a pronounced diurnal cycle signal with distinct regional features. Extreme precipitation is more sensitive to change in DPT at special time periods, indicating that the mix of precipitation from different hours ultimately affects all-hours scaling. This sensitivity could potentially change the diurnal cycle of extreme precipitation under climate change. In the NWC and BTH regions, the current morning sub-peak of extreme precipitation may intensify, narrowing the gap with the afternoon peak, which supports the idea that extreme precipitation may shift to morning and night based on a highresolution convective permitted model (Meredith et al 2019). In addition, by analyzing data from stations with continuous 39 year observations, we found that the variations in EPI correspond with DPT across the diurnal cycle in the inland region. Although 'binning scaling' based on the present-day climate is limited in its ability to extrapolate future extreme precipitation (Zhang et al 2017), current global and regional climate models face challenges in accurately simulating sub-daily extreme precipitation. Nevertheless, the 'binning scaling' approach continues to provide valuable insights into the impacts of climate change on extreme precipitation (Lenderink et al 2018). Our study offers a novel framework for shifts in extreme precipitation to morning/night pattern in some regions under climate change.

Data availability statement

ERA5 and MERRA2 reanalysis data are available from (www.ecmwf.int/en/forecasts/dataset/ecmwf-reanalysis-v5) and (https://disc.gsfc.nasa.gov/datasets/M2T1NXFLX_5.12.4/summary), respectively. The recent hourly rainfall dataset can be downloaded from (http://data.cma.cn/en/?r=data/detail&dataCode=A.0012.0001). Due to the data policy in China, previous data records are not available via a website for public download. However, anyone could contact the China Meteorological Data Service Center (https://data.cma.cn) or the China Meteorological Administration (CMA) (www.cma.gov.cn/en2014/aboutcma/contactus/) for detailed information on data acquisition.

All data that support the findings of this study are included within the article (and any supplementary files).

Acknowledgment

This research was jointly supported by the National Natural Science Foundation of China (grant no.42230611, 42475023, 42075018), and Young Elite Scientists Sponsorship Program by CAST (GXH20220530-09). We would like to thank the ERA5 and MERRA2 science teams for providing excellent and accessible data products that made this study possible.

ORCID iDs

Miao Lei https://orcid.org/0000-0003-1520-3399 Shanshan Wang https://orcid.org/0000-0001-6373-8908

Jianping Huang https://orcid.org/0000-0003-2845-797X

References

- Aleshina M A, Semenov V A and Chernokulsky A V 2021 A link between surface air temperature and extreme precipitation over Russia from station and reanalysis data *Environ. Res. Lett.* 16 105004
- Ali H, Fowler H J, Pritchard D, Lenderink G, Blenkinsop S and Lewis E 2022 Towards quantifying the uncertainty in estimating observed scaling rates *Geophys. Res. Lett.* 49 e2022GL099138
- Ali H, Peleg N and Fowler H J 2021 Global scaling of rainfall with dewpoint temperature reveals considerable ocean-land difference *Geophys. Res. Lett.* 48 e2021GL093798
- Barbero R, Westra S, Lenderink G and Fowler H J 2018
 Temperature-extreme precipitation scaling: a two-way causality? *Int. J. Climatol.* 38 e1274–e9
- Berg P, Haerter J O, Thejll P, Piani C, Hagemann S and Christensen J H 2009 Seasonal characteristics of the relationship between daily precipitation intensity and surface temperature J. Geophys. Res. Atmos. 114 D18102
- Berg P, Moseley C and Haerter J O 2013 Strong increase in convective precipitation in response to higher temperatures *Nat. Geosci.* 6 181–5
- Blenkinsop S, Chan S C, Kendon E J, Roberts N M and Fowler H J 2015 Temperature influences on intense UK hourly

- precipitation and dependency on large-scale circulation Environ. Res. Lett. 10 054021
- Boessenkool B, Bürger G and Heistermann M 2017 Effects of sample size on estimation of rainfall extremes at high temperatures *Nat. Hazards Earth Syst. Sci.* 17 1623–9
- Bui A, Johnson F and Wasko C 2019 The relationship of atmospheric air temperature and dew point temperature to extreme rainfall *Environ. Res. Lett.* 14 074025
- Chen Y, Li W, Jiang X, Zhai P and Luo Y 2021 Detectable intensification of hourly and daily scale precipitation extremes across eastern China *J. Clim.* 34 1185–201
- Craig R K 2010 Stationarity is dead-long live transformation: five principles for climate change adaptation law *Harvard Environ*. Law. **34** 9
- Da Silva N, Mailler S and Drobinski P 2020 Aerosol indirect effects on the temperature–precipitation scaling *Atmos. Chem. Phys.* **20** 6207–23
- Gelaro R, McCarty W, Suárez M J, Todling R, Molod A, Takacs L and Zhao B 2017 The modern-era retrospective analysis for research and applications, version 2 (MERRA-2) *J. Clim.* **30** 5419–54
- Guo J *et al* 2020 The response of warm-season precipitation extremes in China to global warming: an observational perspective from radiosonde measurements *Clim. Dyn.* 54 3977–89
- Guo J, Zhai P, Wu L, Cribb M, Li Z, Ma Z and Zhang J 2014 Diurnal variation and the influential factors of precipitation from surface and satellite measurements in Tibet *Int. J. Climatol.* 34 2940–56
- Hanel M and Buishand T A 2010 On the value of hourly precipitation extremes in regional climate model simulations J. Hydrol. 393 265–73
- Hatsuzuka D, Sato T and Higuchi Y 2021 Sharp rises in large-scale, long-duration precipitation extremes with higher temperatures over Japan *npj Clim. Atmos. Sci.* 4 29
- Herath S M and Sarukkalige R 2018 Evaluation of empirical relationships between extreme rainfall and daily maximum temperature in Australia J. Hydrol. 556 1171–81
- Hersbach H *et al* 2018 ERA5 hourly data on single levels from 1959 to present *Copernicus Climate Change Service (C3S) Climate Data Store (CDS)* (https://doi.org/10.24381/cds. adbb2d47)
- Hosseini-Moghari S M and Tang Q 2022 Can IMERG data capture the scaling of precipitation extremes with temperature at different time scales? *Geophys. Res. Lett.* **49** e2021GL0 96392
- Johnson F and Sharma A 2009 Measurement of GCM skill in predicting variables relevant for hydroclimatological assessments J. Clim. 22 4373–82
- Lehmann J, Coumou D and Frieler K 2015 Increased record-breaking precipitation events under global warming Clim. Change 132 501–15
- Lei M, Li J, Zhang L, Deng C, Li Y and He J 2022 Inconsistent frequency trends between hourly and daily precipitation during warm season in mainland of China *Geophys. Res. Lett.* 49 e2022GL100277
- Lenderink G and Attema J 2015 A simple scaling approach to produce climate scenarios of local precipitation extremes for the Netherlands *Environ. Res. Lett.* **10** 085001
- Lenderink G, Barbero R, Westra S and Fowler H J 2018 Reply to comments on "Temperature-extreme precipitation scaling: a two-way causality?" *Int. J. Climatol.* 38 4664–6
- Lenderink G and Van Meijgaard E 2008 Increase in hourly precipitation extremes beyond expectations from temperature changes *Nat. Geosci.* 1 511–4
- Li J and Heap A D 2008 A review of spatial interpolation methods for environmental scientists (Geoscience Australia) (available at: https://ecat.ga.gov.au/geonetwork/srv/api/ records/a05f7892-db6a-7506-e044-00144fdd4fa6)
- Liu X, Yuan X and Zhu E 2021 Global warming induces significant changes in the fraction of stored precipitation in the surface soil *Glob. Planet Change* 205 103616

- Meredith E P, Ulbrich U and Rust H W 2019 The diurnal nature of future extreme precipitation intensification *Geophys. Res. Lett.* 46 7680–9
- Meredith E P, Ulbrich U, Rust H W and Truhetz H 2021 Present and future diurnal hourly precipitation in 0.11 EURO-CORDEX models and at convection-permitting resolution *Environ. Res. Commun.* 3 055002
- Moustakis Y, Onof C J and Paschalis A 2020 Atmospheric convection, dynamics and topography shape the scaling pattern of hourly rainfall extremes with temperature globally *Commun. Earth Environ.* 1 11
- Ning L, Liu J and Wang B 2017 How does the South Asian High influence extreme precipitation over Eastern China? J. Geophys. Res. Atmos. 122 4281–98
- Pumo D and Noto L V 2021 Exploring the linkage between dew point temperature and precipitation extremes: a multi-time-scale analysis on a semi-arid Mediterranean region *Atmos. Res.* 254 105508
- Qin S, Wang K, Wu G and Ma Z 2021 Variability of hourly precipitation during the warm season over eastern China using gauge observations and ERA5 Atmos. Res. 264 105872
- Roca R 2019 Estimation of extreme daily precipitation thermodynamic scaling using gridded satellite precipitation products over tropical land *Environ. Res. Lett.* 14 095009
- Siswanto S, van Oldenborgh G J, van der Schrier G, Jilderda R and van den Hurk B 2022 Observed increase of urban extreme rainfall as surface temperature rise: the Jakarta case *J. Meteorol. Soc. Japan* II 100 475–92
- Sun Q, Miao C, Duan Q, Ashouri H, Sorooshian S and Hsu K L 2018 A review of global precipitation data sets: data sources, estimation, and intercomparisons *Rev. Geophys*. 56 79–107
- Sun Q, Zwiers F, Zhang X and Li G 2020 A comparison of intra-annual and long-term trend scaling of extreme precipitation with temperature in a large-ensemble regional climate simulation *J. Clim.* 33 9233—45
- Sun W, Yuan W H, Li J and Yu R C 2015 Correlation between peak intensity of extreme afternoon short-duration rainfall

- and humidity and surface air temperature in southeast coast of China *J. Trop. Meteorol.* **21** 276–84
- Sun X and Wang G 2022 Causes for the negative scaling of extreme precipitation at high temperatures *J. Clim.* 35 6119–34
- Tian D, Wood E F and Yuan X 2017 CFSv2-based sub-seasonal precipitation and temperature forecast skill over the contiguous United States *Hydrol. Earth Syst. Sci.* 21 1477–90
- Utsumi N, Seto S, Kanae S, Maeda E E and Oki T 2011 Does higher surface temperature intensify extreme precipitation? *Geophys. Res. Lett.* 38 L16708
- Visser J B, Wasko C, Sharma A and Nathan R 2020 Resolving inconsistencies in extreme precipitation-temperature sensitivities *Geophys. Res. Lett.* 47 e2020GL089723
- Vogel E, Donat M G, Alexander L V, Meinshausen M, Ray D K, Karoly D and Frieler K 2019 The effects of climate extremes on global agricultural yields *Environ. Res. Lett.* 14 054010
- Wang H, Sun F and Liu W 2018 The dependence of daily and hourly precipitation extremes on temperature and atmospheric humidity over China J. Clim. 31 8931–44
- Wang S, Zhang M, Tang J, Yan X, Fu C and Wang S 2024 Interannual variability of diurnal temperature range in CMIP6 projections and the connection with large-scale circulation *Clim. Dyn.* **62** 1–16
- Wasko C, Lu W T and Mehrotra R 2018 Relationship of extreme precipitation, dry-bulb temperature, and dew point temperature across Australia *Environ. Res. Lett.* **13** 074031
- Wu Y, Huang A, Huang D, Chen F, Yang B, Zhou Y and Wen L 2018 Diurnal variations of summer precipitation over the regions east to Tibetan Plateau *Clim. Dyn.* 51 4287–307
- Xiao C, Wu P, Zhang L and Song L 2016 Robust increase in extreme summer rainfall intensity during the past four decades observed in China Sci. Rep. 6 38506
- Yan H, Gao Y, Wilby R, Yu D, Wright N, Yin J and Guan M 2024 Urbanization further intensifies short-duration rainfall extremes in a warmer climate *Geophys. Res. Lett.* 51 e2024GL108565
- Zhang X, Zwiers F W, Li G, Wan H and Cannon A. J. 2017 Complexity in estimating past and future extreme short-duration rainfall *Nat. Geosci.* 10 255–59